Bupivacaine (S75:R25) loaded in Nanostructured lipid carriers: factorial design, HPLC quantification method and…

6 authors, including:

Lígia N.M. Ribeiro
University of Campinas
17 PUBLICATIONS   73 CITATIONS

Viviane Aparecida Guilherme
University of Campinas
23 PUBLICATIONS   76 CITATIONS

Márcia Cristina Breitkreitz
University of Campinas
27 PUBLICATIONS   502 CITATIONS

Eneida de Paula
University of Campinas
211 PUBLICATIONS   2,680 CITATIONS

Some of the authors of this publication are also working on these related projects:

Project   Lipid Nanoparticles View project

Project   Nanostructured Lipid Carrier View project

Research paper

Optimised NLC: a nanotechnological approach to improve the anaesthetic effect of bupivacaine

Gustavo H. Rodrigues da Silva[a], Lígia N.M. Ribeiro[a], Hery Mitsutake[b], Viviane A. Guilherme[a], Simone R. Castro[a], Ronei J. Poppi[b], Márcia C. Breitkreitz[b], Eneida de Paula[a,*]

[a] Department of Biochemistry and Tissue Biology, Institute of Biology, University of Campinas, UNICAMP, Campinas, São Paulo, Brazil
[b] Department of Analytical Chemistry, Institute of Chemistry, University of Campinas, UNICAMP, Campinas, São Paulo, Brazil

ABSTRACT

The short time of action and systemic toxicity of local anaesthetics limit their clinical application. Bupivacaine is the most frequently used local anaesthetic in surgical procedures worldwide. The discovery that its S(−) enantiomeric form is less toxic than the R(+) form led to the introduction of products with enantiomeric excess (S75:R25 bupivacaine) in the market. Nevertheless, the time of action of bupivacaine is still short; to overcome that, bupivacaine S75:R25 (BVC$_{S75}$) was encapsulated in nanostructured lipid carriers (NLC). In this work, we present the development of the formulation using chemometric tools of experimental design to study the formulation factors and Raman mapping associated with Classical Least Squares (CLS) to study the miscibility of the solid and the liquid lipids. The selected formulation of the nanostructured lipid carrier containing bupivacaine S75:R25 (NLC$_{BVC}$) was observed to be stable for 12 months under room conditions regarding particle size, polydispersion, Zeta potential and encapsulation efficiency. The characterisation by DSC, XDR and TEM confirmed the encapsulation of BVC$_{S75}$ in the lipid matrix, with no changes in the structure of the nanoparticles. The *in vivo* analgesic effect elicited by NLC$_{BVC}$ was twice that of free BVC$_{S75}$. Besides improving the time of action, no statistical difference in the blockage of the sciatic nerve of rats was found between 0.125% NLC$_{BVC}$ and 0.5% free BVC$_{S75}$. Therefore, the formulation allows a reduction in the required anaesthesia dose, decreasing the systemic toxicity of bupivacaine, and opening up new possibilities for different clinical applications.

© 2017 Elsevier B.V. All rights reserved.

1. Introduction

Pain is one of the most extensively studied issues in medicine. Local anaesthetics (LA) are capable of blocking nerve impulse conduction, reversibly abolishing the painful sensation. LA are especially used in the prevention of surgical pain, despite their limited performance in the control of postoperative, chronic and neuropathic pain. However, LA time of action is short (1–4 h), requiring the drug to be administered more than once. Another limitation of the use of local anaesthetics is their systemic (mainly cardiac and neurological) toxicity (Harmatz, 2009; Mather and Chang, 2001). Thus, there is still a need for the development of novel anti-nociceptive formulations to prolong the time course of available LA and to decrease their systemic toxicity.

The development of drug delivery systems (DDS), such as nanostructured lipid carriers (NLC), opened up the possibility of finding solutions to these problems. NLC are the second generation of solid lipid nanoparticles. They are composed of a mixture of solid and liquid lipids at room temperature, thereby presenting improved active loading and stability compared to solid lipid nanoparticles (Müller et al., 2011, 2007). NLC benefits include versatility (they can be used by several routes of administration), safety (due to the use of biocompatible and functional excipients with reduced cytotoxicity) (Joshi and Müller, 2009; Müller et al., 1996) and low cost, making them attractive for the pharmaceutical and cosmetic industries (Battaglia and Gallarate, 2012; Puglia et al., 2011).

* Corresponding author at: Department of Biochemistry and Tissue Biology, Institute of Biology, University of Campinas, UNICAMP, Rua Monteiro Lobato, 255, Cid. Universitária Zeferino Vaz, Campinas, São Paulo, Brazil.
 E-mail address: depaula@unicamp.br (E. de Paula).

Bupivacaine (Fig. S1A) is an amine-amide local anaesthetic, with two optical isomers: levobupivacaine S(−) and dextrobupivacaine R(+). It is extensively used for surgical procedures (e.g. caesarean section) and in the postoperative period, with a half-life of 4 to 6 h (Covino, 1986; Lagan and McLure, 2004). Because of the more pronounced cardiotoxicity of the (R) enantiomer (Bergamaschi et al., 2005) a formulation has been developed for clinical use (by Cristália Prod. Quim. Farm. Ltda) called Novabupi®, with an excess of the S(−) enantiomeric form (S = 75%, R = 25%), herein called BVC$_{S75}$, to decrease the anaesthetic toxicity (de Araújo et al., 2005; Bergamaschi et al., 2005).

The present work aimed at developing a formulation of BVC$_{S75}$ loaded in NLC to overcome the above-mentioned clinical drawbacks associated to bupivacaine. After the selection of the lipids, based on a miscibility study carried out by Raman mapping, an optimisation by experimental design was performed. The optimised formulation was then characterised by transmission electron microscopy (TEM), differential scanning calorimetry (DSC) and powder X-Ray diffraction (XDR) and the stability was studied over 12 months. Release kinetics was tested in vitro while the analgesic effect tests we performed using the paw pressure test (Randall and Selitto, 1957) in rats. In vivo tests confirmed the improved anaesthetic effect (>8 h) of the optimized NLC$_{BVC}$ formulation, which carries the potential to be used in several administration routes, such as topical and parenteral.

2. Materials and methods

2.1. Materials

Bupivacaine S75:R25 (BVC$_{S75}$) was donated by Cristália Prod. Quim. Farm. Ltda (Brazil). Cetyl Palmitate (CP) and Dhaykol 6040® (DK) were purchased by Dhaymers Química Fina (Brazil), Capryol 90® (CAP) and Precirol ATO5® (PRE) were obtained by Gattefossé (France). The surfactant Pluronic® F68 (P68) was supplied by Sigma (USA). Deionised water (18 MΩ) was obtained from an Elga USF Maxima ultra-pure water purifier.

2.2. Pre-formulation study: Raman mapping and chemometric method applied to Raman image treatment

The preparation of lipid mixtures was achieved by heating the solid lipids (CP, PRE) 10 °C above their respective melting points and adding the liquid lipid (CAP, DK) under stirring, until a visually homogeneous mixture was obtained. The proportion of solid and liquid lipids was 70:30% (w/w) for the systems CP-CAP, CP-DK and PRE-CAP. The samples were cooled to room temperature in an aluminium cell and an area of 1.95 × 1.95 mm^2 was mapped, using a Raman Station 400 spectrometer (PerkinElmer, CT, USA). The exposure time was 3s/pixel and 2 exposures were taken; the size of the pixel was 50 μm and the spectral range was set to 600–3200 cm^{-1}, with a resolution of 4 cm^{-1}. Pure spectra of excipients were used for Classical Least Squares (CLS) model calculations. Thus, each data cube has the dimension of 40 × 40 × 651, where the first two numbers represent the number of pixels in the directions x and y (i.e., positions of pixels) and the last is the spectral variable.

The Raman spectra were corrected before building the models. The spikes were removed from spectra using an algorithm written in Matlab (Sabin et al., 2012). After this, the data cube was unfolded in a 2D matrix, where each row was a spectrum and each column was a spectral variable, providing a data matrix of 1600 × 651 dimensions. The baseline offset was corrected using the Weighted Least Squares baseline function that subtracts a baseline from a spectrum using an iterative asymmetric least squares algorithm.

The normalisation by unit vector was used to remove spectral intensity differences due to physical effects, such as the difference in the laser focus and superficial roughness.

Classical Least Squares (CLS) is a simple and very useful method for the analysis of pharmaceuticals since it requires only the spectra of pure components to build the model. This method assumes that spectra of mixtures result from the weighted sum (by their concentration) of all pure component spectra. It can be represented in a matrix form, by Eq. (1):

$$D = CS^T + E \qquad (1)$$

where D is data matrix containing the mixture spectra, C is concentration profile, S is pure spectra and E is matrix error.

A spectral region was selected for each mixture based on the average prediction error. In the case of CP mixtures, the models were built using the 2964–724 cm^{-1} spectral range, while for mixtures containing PRE, the best model was built using the 1804–724 cm^{-1} range. After applying CLS in the data, the predicted concentrations for excipients were refolded in concentration maps (the chemical images) and histograms of these concentrations were generated. Data analyses were performed using Matlab® R2014a (Mathworks Inc., Natick MA, USA) and PLS Toolbox® version 7.3.1 (Eigenvector Research Inc., Wenatchee WA, USA).

2.3. NLC preparation method

NLC formulations were prepared by the emulsification-ultra-sonication method (Schwarz et al., 1994). Briefly, a blend of solid and liquid lipids and BVC$_{S75}$ are melted in a water bath 10 °C above to the melting point of the solid lipid (CP = 55.0 °C (Ribeiro et al., 2016) and PRE = 56.0 °C (Patil-Gadhe and Pokharkar, 2014). The aqueous phase, a solution of Pluronic F68 (P68), was heated to the same temperature. Both phases were blended under high-speed agitation (10,000 rpm), for 3 min in an Ultra-Turrax blender (IKA WerkeStaufen, Germany). After, the mixture was sonicated for 30 min using a Vibracell tip sonicator (Sonics & Mat. Inc., Danbury, USA) operated at 500 W and 20 kHz, in alternating 30 s (on and off) cycles. The resultant nanoemulsion was immediately cooled to room temperature with an ice bath.

2.4. Experimental design

A 2^4 experimental design with central points in triplicate was performed for optimisation of the NLC formulation. The Design Expert® software (version 9.0.6.2, Stat-Ease Inc., USA) was used for the analysis of results. Analysis of Variance (ANOVA) was applied to verify the adjusted model and was considered significant if the p value was less than 0.05 (Carbone et al., 2012). The variables, levels and responses are listed in Table 1.

Table 1
Experimental variables, levels, responses and optimizing goals for the 2^4 experimental design.

Variable	Low Level	High Level
Cetyl Palmitate (%w/w)	5	9
Capryol 90® (%w/w)	1	5
Pluronic® F-68 (%w/w)	2.5	5
Bupivacaine S75-R25 (%w/w)	0.5	1.5

Response	Goal
Particle size (nm)	Minimum
Polydispersity index (PDI)	Minimum
Zeta Potential (|mV|)	Maximum

2.5. Nanoparticles characterisation

2.5.1. Particle size, polydispersity, zeta potential and nanoparticle concentration determination

A dynamic light scattering (DLS) equipment (Nano ZS90 analyser – Malvern Instruments, UK) was used to determine the hydrodynamic radius (size), polydispersity index (PDI) and zeta potential (ZP) of the nanoparticles. For determination of the number of particles in the formulation, an NS300 Nanotracking analysis instrument (NanoSight, Amesbury, UK), equipped with a 532 nm laser was used. In both cases, samples were diluted in deionised water (n = 3).

2.5.2. Bupivacaine quantification: encapsulation efficiency (%EE) and drug loading

The quantification of BVC_{S75} was performed by high performance liquid chromatography (HPLC) using a Varian ProStar HPLC (equipped with a PS 325 UV–Vis detector, a PS 210 solvent delivery module and Galaxy Workstation software for data collection). The column was a Gemini$^{®}$ 5 μm, C18, 110 Å, with 150 × 4.6 mm (Phenomenex$^{®}$, Torrance, USA) with flux of 1 mL min^{-1}. The mobile phase was composed of a mixture (70:30:0.1, v/v) of water, acetonitrile and phosphoric acid. The injection volume was 30 μL and the absorbance was followed in 210 nm. The total amount (100%) of BVC_{S75} present in the nanoparticle suspension was determined by diluting the samples in the mobile phase (n = 3) (Moraes et al., 2008). The BVC_{S75} encapsulation efficiency (%EE) was determined by the ultrafiltration-centrifugation method, using cellulose filters (30 kDa, Millipore). The amount of free BVC_{S75} in the filtrates was quantified by HPLC and the percentage of encapsulated BVC were calculated according to Eq. (2) (Araújo et al., 2010; Moraes et al., 2008; Teeranachaideekul et al., 2007):

$$\%EE = \frac{BVC_{total} - BVC_{free}}{BVC_{total}} \times 100 \tag{2}$$

Alternatively, the amount of BVC_{S75} uploaded in the nanoparticles was expressed in drug loading (%), accordingly to Eq. (3) (Chen et al., 2015; Nahak et al., 2015):

$$\%Drug\ loading = \frac{weight\ of\ encapsulated\ BVC}{weight\ of\ nanoparticles} \times 100 \tag{3}$$

2.5.3. Transmission electron microscopy

Morphological analysis was carried out for the optimised NLC formulations (those composed of CP and CAP), with and without BVC_{S75} by transmission electron microscopy (TEM). Uranyl acetate (2%) was added to the diluted samples providing contrast. Then, the aliquots were deposited onto copper grids coated with a carbon film and dried at room temperature. After drying, micrographs of the samples were appreciated using a JEOL 1200 EXII microscope operated at 80 kV.

2.5.4. Differential scanning calorimetry (DSC)

DSC thermograms of the optimised NLC formulations were collected in a 2910 Model calorimeter (TA Instruments, DE, USA) and analysed with Thermal Solutions v.1.25 (TA Instruments, DE, USA) software. The samples were dried and heated at the rate of 10 °C min^{-1}, with the temperature ranging from 20 to 150 °C. Samples of nanoparticles prepared without (NLC$_{FREE}$) and with bupivacaine (NLC$_{BVC}$), besides their main components (CP and BVC_{S75}) were run.

2.5.5. X-ray diffraction analysis (XDR)

Powder X-ray diffraction (XRD) data were obtained in a Shimadzu XRD7000 diffractometer (Tokyo, Japan), using a Cu-Kα source, with a scan step of 2° min^{-1}, between 2θ values (5 and 50°). Samples of the optimised NLC formulations, prepared without (NLC$_{FREE}$) and with bupivacaine (NLC$_{BVC}$) and their main components (CP and BVC_{S75}) were run.

2.6. Physicochemical stability study

The physicochemical stability of NLC formulations was monitored during 12 months, at room temperature (25 ± 2 °C; 60 ± 5% humidity) (Ribeiro et al., 2016). The analysed parameters were: nanoparticle size (nm), PDI, ZP (mV) and %EE. Analysis of variance (ANOVA, 95% confidence level) and Tukey post hoc test were used to compare inter-groups significant differences, regarding the initial time measurements.

2.7. Release kinetics experiments

The in vitro release of BVC_{S75} in solution or loaded in NLC (NLC$_{BVC}$) was studied using a Franz diffusion cell system, with 5 mM PBS buffer (pH 7.4, 37 °C) as the donor solution, separated by a polycarbonate membrane (Nucleopore Track-Etch, 19 mm diameter, 0.1 μm pore size, Whatman$^{®}$) (n = 6) (Tiyaboonchai et al., 2007). Serial sampling was performed at specified time intervals (0.15, 1, 2, 4, 6, 8, 22, 24, 28 h) by removing 200 μL of the receptor compartment and replacing it with the fresh medium, to maintain the sink condition. The amount of BVC_{S75} in the acceptor compartment was quantified by HPLC. The KinetDS 3.0 software was used for the quantitative analysis of the obtained release curves (Mendyk et al., 2012); several kinetic models were tested and, according to the R^2 coefficient, the Korsmeyer-Peppas (Eq. (4)) presented the best fit.

$$Q = k.t^n \tag{4}$$

where Q is the fraction of drug liberation, k is the constant, t is the time of release and n, the release exponent.

2.8. In vivo analgesia tests

Adult male Wistar rats (Rattus novegicus albinus) (250–350 g) were obtained from CEMIB-UNICAMP (Centro de Bioterismo/ UNICAMP). The experimental protocol was approved by the UNICAMP Institutional Animal Care and Use Committee (protocol #4155-1), which follows the recommendations of the Guide for the Care and Use of Laboratory Animals. The rats were randomly divided in batches of 5 animals, which were treated by injection of 0.2 mL of each formulation into the popliteal space, posterior to the knee joint, in the sciatic nerve area (de Melo et al., 2011). The injected formulations were free BVC_{S75} and NLC$_{BVC}$ with bupivacaine concentrations of 0.125 and 0.5%.

Sensory blockade evaluation was performed by the paw pressure test (Randall and Selitto, 1957) using an analgesimeter (Ugo Basile, Varese, Italy). The withdrawal reflex was considered representative of the pain threshold or Paw Withdrawal Threshold to Pressure (PWTP), taking into account the registered force (in grams) on the injected paw. The baseline of the PWTP test was measured before the injections, in order to determine the pain threshold of the animal. Baseline values of 30–50 g were selected as the pain threshold, and animals that presented lower or higher values than that baseline were excluded. The established nociceptive cut-off value was 180 g, considered to be representative of the anaesthetic state. After treatment, the first measurement was carried out at 30 min, and after that, in intervals of one hour until 11 h. The obtained values were transformed into data of maximum possible effect (% MPE), according to Eq. (5) (Penning

and Yaksh, 1992).

$$\%MPE = \frac{(treshold - baseline)}{(cutoff - baseline)} \times 100 \qquad (5)$$

where %MPE is the percentage of maximum possible effect, threshold corresponds to the pressure values, baseline is the standard value of each animal, and cut-off refers to the limit (180 g) pressure to avoid skin injury.

The area under the curve (AUC) of analgesic effect was calculated through the %MPE plot. Statistical analyses were performed by One-Way ANOVA with Tukey-Kramer post-test, using GraphPad Prism version 6.00 for Windows (California, USA).

3. Results

The selection of a suitable composition of the lipid matrix is the first step to success in the development of NLC. Several types of lipid mixtures have been described in the literature for NLC preparation, which are compatible with biomedical applications (Müller et al., 2000). The main criterion for the choice is the solubility of the drug in the lipid matrix. The liquid lipids that best solubilised BVC_{S75} were Capryol 90® and Dhaykol 6040® (data not showed). With these lipids, empirical test formulations based on prior knowledge of the group (Ribeiro et al., 2016) and using the solid lipids CP and PRE were run (see Supplementary material – Figs. S1D and E). The CP-CAP, CP-DK and PRE-CAP mixtures gave rise to liquid formulations, which were versatile for several routes of administration (Doktorovová et al., 2016) (Table S1). To obtain more information about these mixtures of lipids, Raman mapping was performed, allowing for a better understanding of the homogeneity and miscibility of these lipid mixtures, chosen through empirical tests.

3.1. Raman mapping and chemometric analysis

Spectra of excipients and mixtures are shown in Fig. 1. The spectrum of cetyl palmitate was similar to that found in the literature, with two characteristic bands at 2880 and 2850 cm^{-1} (ν_{as} CH$_2$ and ν_{s} CH$_2$, respectively) (Anantachaisilp et al., 2010a; Saupe et al., 2006); other important bands were found at 1444, 1296, 1128 and 1064 cm^{-1}. The Raman spectrum of DK shows bands at 2912, 2860, 2732, 1744, 1444, 1304, 1116, 1036, 888 and 840 cm^{-1} and is similar to that reported in a former publication

(Anantachaisilp et al., 2010a; Sütő et al., 2016), while the main bands of CAP are assigned at 2932, 2732, 1736, 1448, 1304, 1116, 1072, 896 and 844 cm^{-1}. PRE bands lie at 2880, 2852, 2728, 1444, 1296, 1128, 1064 and 888 cm^{-1}. The strong peaks that appear to all spectra in the region 2932 to 2843 cm^{-1} refer to —CH$_3$ and —CH$_2$— bonds. Other bands related to —CH$_3$ bonds are found at 1064 cm^{-1} in the cetyl palmitate spectrum (Patnaik, 2004). All excipient spectra showed peaks at 1304 to 1296 cm^{-1}, which are attributed to —CH$_2$ bonds. The peaks at 2732 and 2728 cm^{-1} in liquid lipids are related with —CH bond. The band at 1444 and 1448 cm^{-1} in all excipient spectra refer to —CH$_2$ bonds (Patnaik, 2004). The ν —C=O bond in esters is represented by a weak band encounter in 1744 and 1736 cm^{-1} in the spectra of DK and CAP (Patnaik, 2004). The peak at 1304 cm^{-1} encountered in the DK spectrum was considered characteristic of this compound (Anantachaisilp et al., 2010b). The medium peaks of 1128 and 1064 cm^{-1} in CP and PRE were attributed to ordered acyl chains in the lipid structure (Sütő et al., 2016). Peaks around 890 to 830 cm^{-1} represent R—O—R in aliphatic acyclic compounds (Patnaik, 2004) and were encountered for all excipients, except cetyl palmitate. The peak at 1072 cm^{-1} in the CAP spectrum was attributed to C—O bond (Patnaik, 2004).

Univariate methods can be used to construct chemical images (Breitkreitz et al., 2013) y selecting specific peaks or spectral regions (e.g. 845 cm^{-1} for CAP or 1750 cm^{-1} for DK), but the multivariate CLS method has the advantage of using the information contained in the entire spectrum, providing superior results in terms of concentration prediction and therefore, providing more reliable chemical images.

The chemical images and histograms obtained for each excipient in the mixtures are shown in Fig. 2. Each pair of solid and liquid lipids is shown on the right and left sides, respectively, of Fig. 2A–C. The parameters used for evaluating these models were absolute error (real concentration−predicted mean concentration) in each map and complementary of the maps, i.e., the sum of the concentrations of each excipient in every pixel should be close to the unit. To evaluate the homogeneity of these formulations, the standard deviation (SD) of histograms were compared.

The average predicted concentration and concentration ranges for each component in the pixels are listed in Table S2. The absolute error of CP-CAP mixture was higher than the others, which could be due to the normalisation step of pure spectra, which generates intensity ambiguity in the CLS method (Tauler et al., 1995). In this
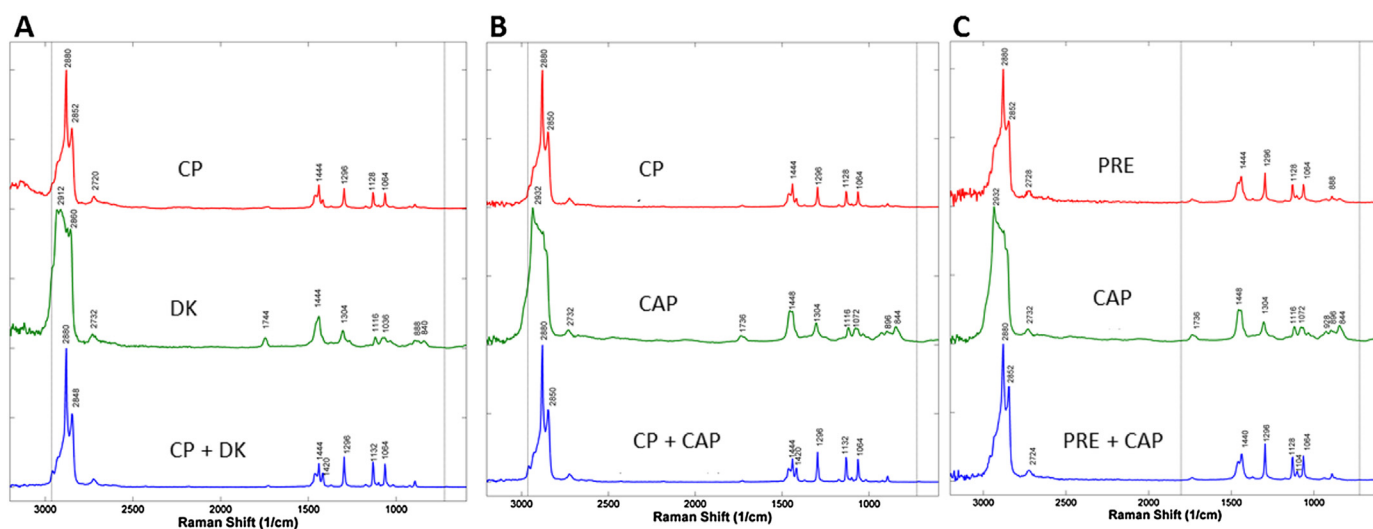
Fig. 1. Raman spectra of lipids and their mixtures: (A) Cetyl palmitate [CP] and Dhaykol [DK]; (B) Cetyl palmitate [CP] and Capryol [CAP] and (C) Precirol [PRE] and Capryol [CAP]. Solid lipid excipient spectra (on top), liquid lipid spectra (medium) and mean spectra of their mixtures (bottom).
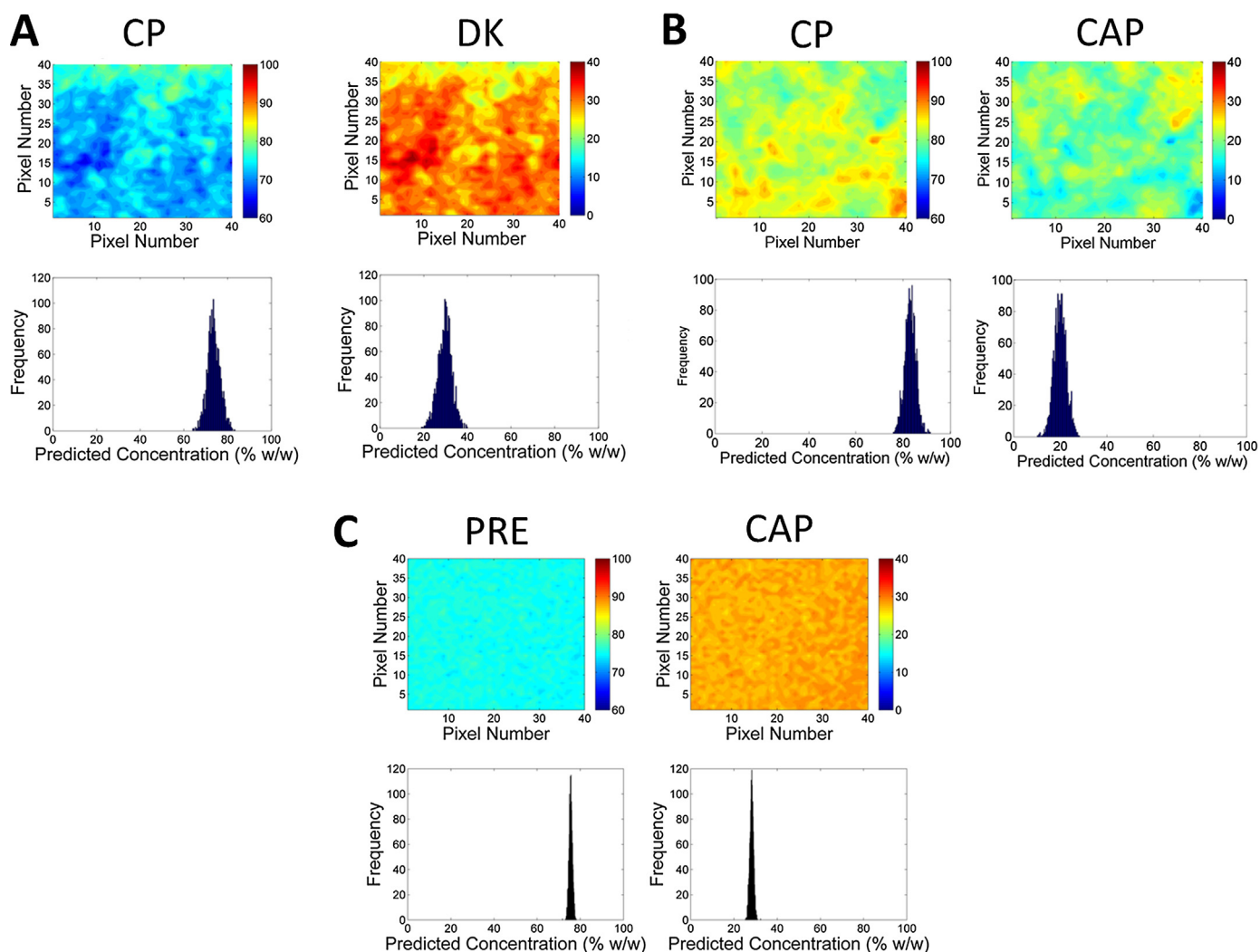
Fig. 2. Raman images: distribution maps and histograms of predicted values for: (A) Cetyl palmitate [CP] and Dhaykol [DK]; (B) Cetyl palmitate [CP] and Capryol [CAP] and (C) Precirol [PRE] and Capryol [CAP]. Solid (CP, PRE) lipids are shown on the right and liquid lipids (DK, CAP) are shown in the left sides.

way, the predicted concentrations are shifted in the X axis, but the chemical maps represent the real distribution of components in the mixture and SD can be used for comparison with the other mixtures. SD values of 2.5, 3.0 and 0.8 were determined for CP-CAP, CP-DK and PRE-CAP, respectively. Pixels presenting 0 or 100% concentration values of the components that would indicate immiscibility between them were not observed in any of the mixtures. From these image analyses, we could conclude that the three mixtures presented reasonable miscibility between the solid and liquid lipid excipients, with a homogeneity profile, from the histograms, of: PRE-CAP > CP-CAP > CP-DK.

Thus, the two mixtures containing CAP as the liquid lipid could be used for the continuation of the studies because they present the better homogeneity. However, the formulation containing PRE as the solid lipid presented phase separation (precipitate

formation) after one month of preparation, indicating instability over time, possibly due to its polymorphic modification (Kasongo et al., 2011). The CP-CAP mixture was then selected as the best lipid composition towards an optimised formulation. From this point, an experimental design approach was performed to find the best proportion among the components of the CP-CAP formulation, and to understand how each of the factors would affect the final formulation.

3.2. Experimental design

Experimental Design is a multivariate tool to determine the influence of the factors of the formulation on the quality criteria and it is recommended by the ICH in Quality by Design approach (ICH, 2009; Patil and Pethe, 2013; Sangshetti et al., 2017). A 2^4

Table 2
Summary of responses obtained in the 2^4 experimental design, with the range of values and significant factors. Nanoparticles size, polydispersity and zeta potential were determined by DLS.

Response	Range of values	Significant factor with positive effect	Significant factor with negative effect
Size	107.1 to 303.7 nm	CP	CAP and P68
PDI	0.115 to 0.242	BVC	CAP and P68
ZP	-14.5 to -41.5 mV	–	P68

experimental design with central points was carried out for the NLC system totalling 19 formulations. The description of variables and responses is presented in Table S3. The quality criteria used as responses were particle size, PDI and zeta potential of the nanoparticles (Ribeiro et al., 2017, 2016; Shah et al., 2014). The linear polynomial models generated to establish the relation between the components of the formulation and the responses presented no lack of fit. Table S4 shows the *p*-values for the regression significance (model) and lack of fit. Table 2 shows a range of obtained values for each response and the significant factors that changed the response, which graphics of response surface are depicted in Fig. 3. The complete statistical analysis can be found in Tables S5–S7. As can be seen in these tables, many interaction coefficients are significant, which shows the importance of the use of a multivariate method, instead of the univariate approach of changing one factor at a time.

The desirability region (Fig. S2) was determined based on the goal for each response, as described in Table 1. Considering those criteria, the optimal formulation selected was composed of 9% CP, 4% CAP, 5% P68 and 1% BVC$_{S75}$ (w/w) and the next experiments were conducted with NLC prepared with this composition. Table 3 shows the response values (size, PDI, and ZP), % EE and number of particles, obtained from the optimal formulation.

3.3. Transmission electron microscopy

Information about the morphology of nanoparticles can be obtained by transmission electron microscopy (Garg et al., 2017; Hu et al., 2005; Mohanty et al., 2015). Fig. 4 (A and C) shows spherical nanoparticles with regular and defined borders. The

addition of BVC$_{S75}$ did not change NLC morphology (Nahak et al., 2015; Ribeiro et al., 2016) (Fig. 4B and D). Moreover, the observed nanometric sizes of the nanoparticles were compatible with those determined by DLS (Table 3).

3.4. Differential scanning calorimetry and X-ray diffraction analysis

In order to characterise the lipid matrix of NLC and to correlate it with drug encapsulation, DSC and XRD analyses were conducted (Rute Neves et al., 2013). Fig. 5A shows the thermograms of pure CP and BVC$_{S75}$, SLN (composed of 9% CP and 5% P68), NLC$_{FREE}$ and NLC$_{BVC}$. For the NLC$_{FREE}$ samples only one peak of fusion (relatively to CP) is seen, since the solid lipid is the component of the higher amount in the system (Martins et al., 2012). The melting point of CP decreased from 57.5 °C to 53.9 °C in NLC$_{FREE}$ and 54.6 °C in NLC$_{BVC}$. The enthalpy decreased from 179.1 J/g in solid lipid nanoparticles (SLN) to 96.9 J/g NLC$_{FREE}$ and 79.9 J/g for NLC$_{BVC}$. The peak of BVC$_{S75}$ was not observed in NLC$_{BVC}$, suggesting that a structural rearrangement in the lipid core was caused by the addition of the liquid lipid and the drug. Both CAP and BVC$_{S75}$ were probably inserted in the lipid core of the nanoparticles.

X-ray diffraction (XDR) is a technique that can give information about polymorphic changes in the crystallinity of the lipid nanoparticles (Bunjes, 2011) and complement the DSC analysis. The results obtained for SLN, NLC$_{FREE}$, NLC$_{BVC}$ and their components are shown in Fig. 5B. The diffractogram of pure CP shows intense peaks at 7, 11, 21 and 24°, evidencing the high degree of crystallinity of the pure lipid (Ruktanonchai et al., 2008). These peaks decreased in intensity when CP was in NLC$_{FREE}$ and NLC$_{BVC}$, indicating that both the addition of liquid lipid and BVC$_{S75}$ destabilised the molecular organisation of the CP, which is
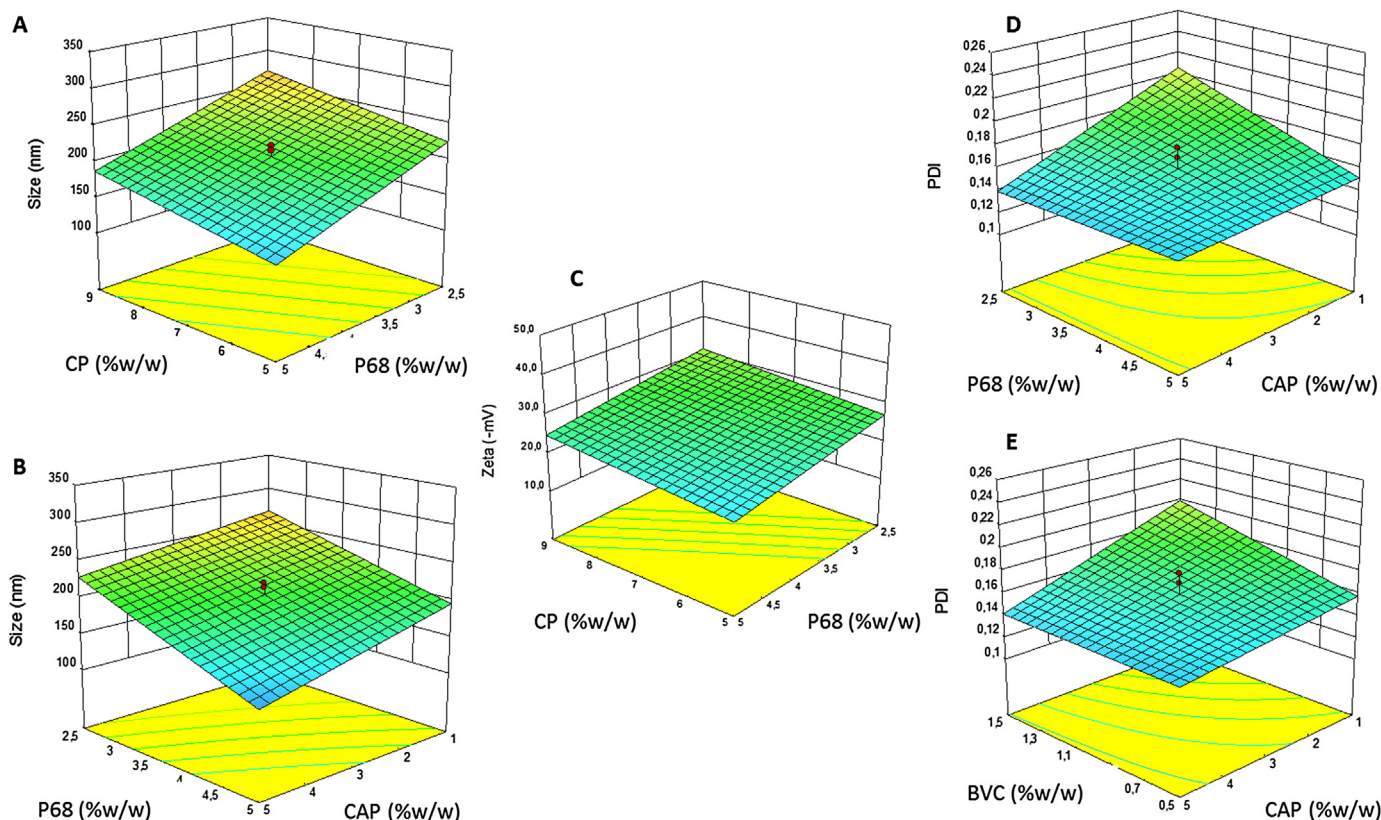
Fig. 3. Response surfaces for size (A, B), zeta potential (C) and PDI (D, E).

Table 3

Response values for the optimised NLC formulation (composed of 9% CP, 4% CAP, 5% P68 w/w). NLC_{FREE} = nanostructured lipid carriers without bupivacaine S75:R25 and NLC_{BVC} = nanostructured lipid carriers with 1% bupivacaine S75:R25.

Formulations	Size (nm)	PDI	ZP (mV)	%EE ± SD	Number of particles/mL
NLC_{FREE}	156.0 ±2.5	0.123 ±0.009	−15.7 ±0.6	–	$7.4 \times 10^{13} \pm 4.06 \times 10^{12}$
NLC_{BVC}	165.9 ±1.5	0.123 ±0.005	−37.0 ±1.1	55.5 ±3.6	$8.8 \times 10^{13} \pm 1.11 \times 10^{12}$
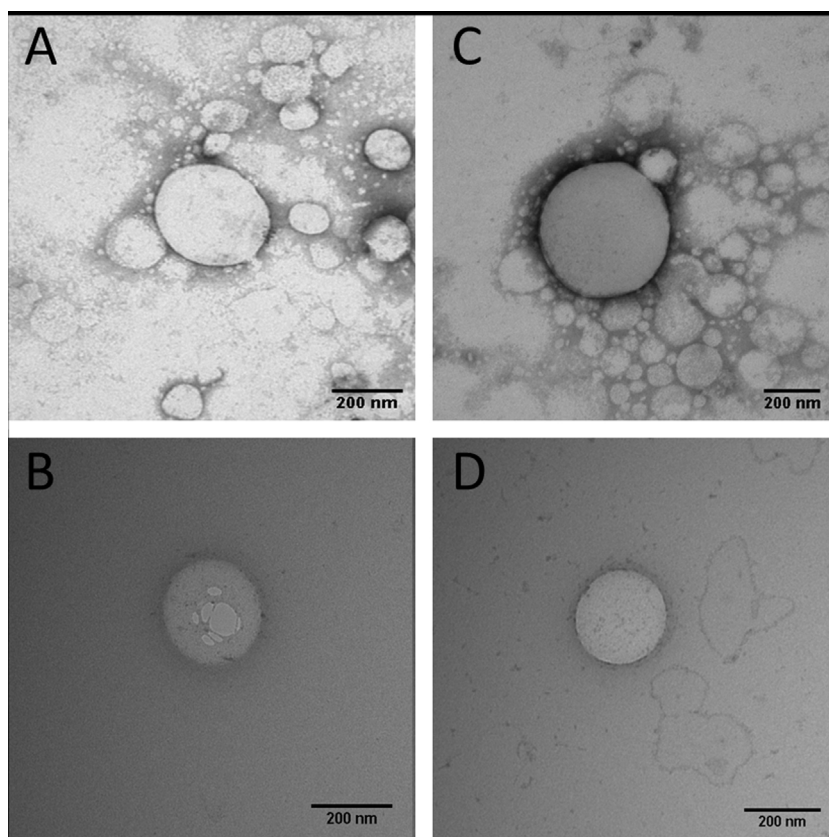
Fig. 4. TEM images of the optimised NLC formulation without (A, B) and with bupivacaine (C, D). Magnification: 60,000× (A, C) and 100,000× (B, D) Scale bar = 200 nm.
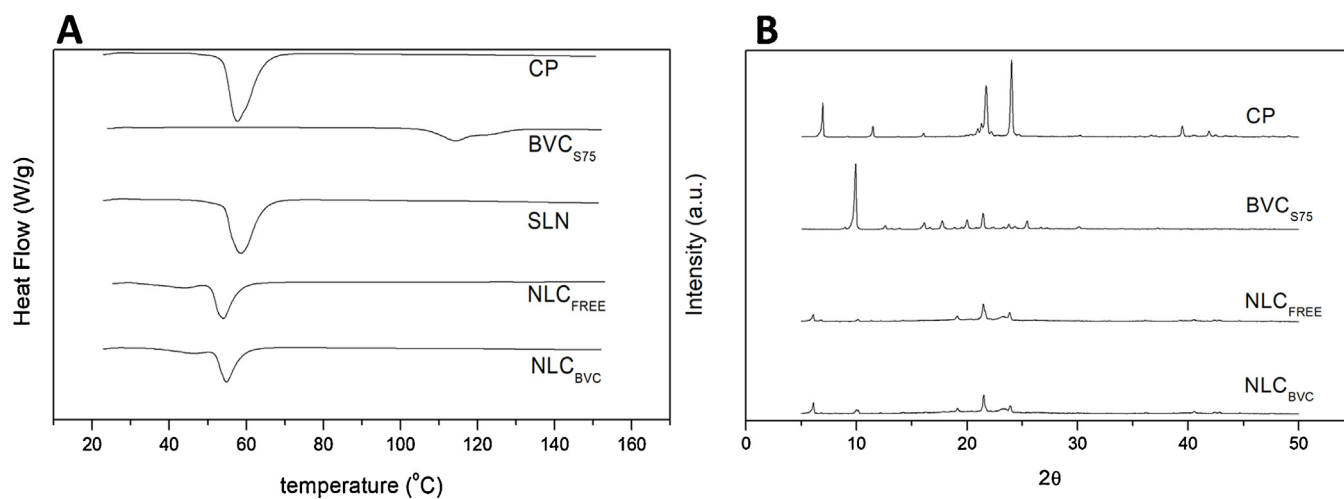
Fig. 5. (A) DSC results on the optimised nanostructured lipid carriers (without = NLC_{FREE}, and with = NLC_{BVC} bupivacaine), solid lipid nanoparticles (SLN) composed of 9% CP and 5% P68 without bupivacaine and their pure components (CP and BVC_{S75}); thermograms obtained at a heating rate of 10 °C min^{-1}. (B) XRD analyses for NLC_{FREE}, NLC_{BVC}, CP and BVC_{S75} obtained with a Cu-Kα source, at a scan step of 2° min^{-1}.

expected for the formulation (Gonzalez-Mira et al., 2011; Neupane et al., 2014). In addition, the diffraction pattern of powder BVC_{S75}, with a high intensity peak at 10° is in agreement with the literature (for racemic bupivacaine, (Cheung et al., 2004) attesting the crystalline form of the pure anaesthetic.

3.5. Physicochemical stability study

Physicochemical stability studies should be performed in NLC formulations because the lipid components may suffer polymorphic modifications and destabilise the system (Gonzalez-Mira et al., 2011; Souto et al., 2004; Vivek et al., 2007) as a function of time. Thus, to follow the physicochemical stability the optimised formulation without BVC_{S75} (NLC_{FREE}) and with BVC_{S75} (NLC_{BVC}) they were stored at room temperature and studied for 12 months, considering the parameters size, PDI, zeta potential and %EE. The results obtained are shown in Fig. 6 and Table S8. No statistically significant differences were observed for any of the analysed parameters, in comparison to the initial values. Moreover, to confirm the stability of the nanoparticles arrangement during storage, a XDR diffractogram was run in a NLC_{BVC} sample stored for 17 months at room temperature. In comparison to a freshly prepared sample, no increase in the crystallinity was detected as shown in Fig. S3 (Supplementary materials).

3.6. Release kinetics

NLC formulations have a biodegradable matrix with temperature-dependent properties, that favour the drug release (Abdel-Mottaleb et al., 2010), as confirmed in this study. Results of the *in vitro* release experiments are shown in Fig. 7. The solution of BVC_{S75} released 100% of the anaesthetic after 1 h of the experiment,
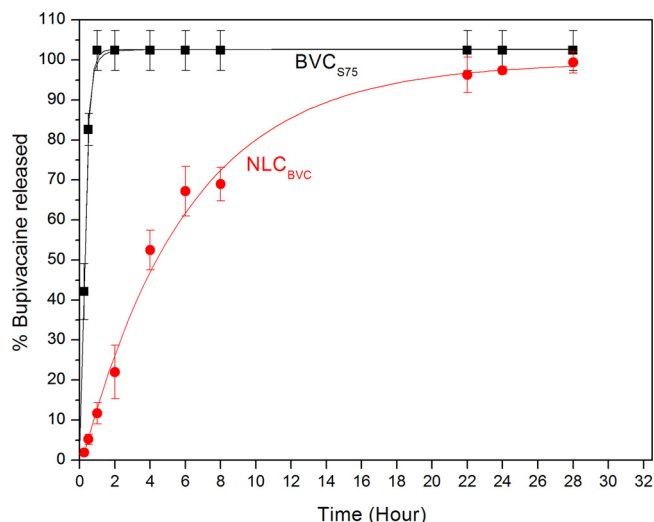
Fig. 7. *In vitro* release profiles of Bupivacaine S57:R25 in solution (BVC_{S75}) and encapsulated in the optimised nanostructured lipid carriers (NLC_{BVC}) (n = 6).

while the NLC_{BVC} formulation showed a prolonged release profile with complete bupivacaine release after 28 h. Analysis of the release curves using mathematical models (zero order, first order, Higuchi, Hixson-Crowell and Korsmeyer-Peppas) current in the KinectDS3 software showed that Korsmeyer-Peppas was the best-fit model, considering the R^2 values (Table S9). According to the n exponent (0.8) of the Korsmeyer-Peppas model (Eq. (4)), the release mechanism of the anaesthetic from the optimised NLC_{BVC} formulation was defined as non-Fickian anomalous transport (Korsmeyer et al., 1983).
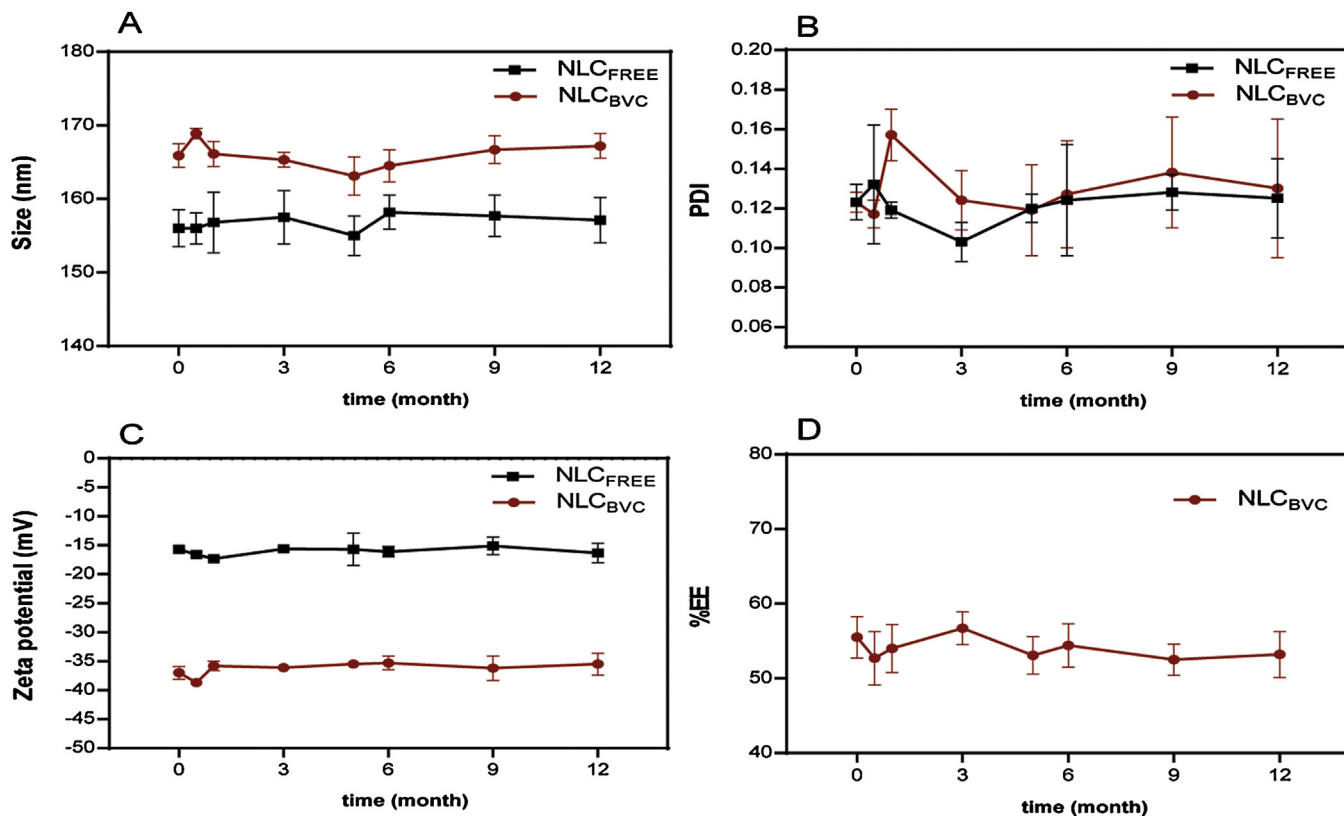
Fig. 6. Stability study of the optimised NLC formulation: without BVC_{S75} (NLC_{FREE}) and with BVC_{S75} (NLC_{BVC}) considering size (A); PDI (B), zeta potential (C) and encapsulation efficiency, %EE (D) during 12 months of storage. NLC formulations were composed of 9% CP, 4% CAP and 5% P68 plus 1% BVC (w/w). The statistical analysis results indicate no statistically significant differences in comparison to the initial results.
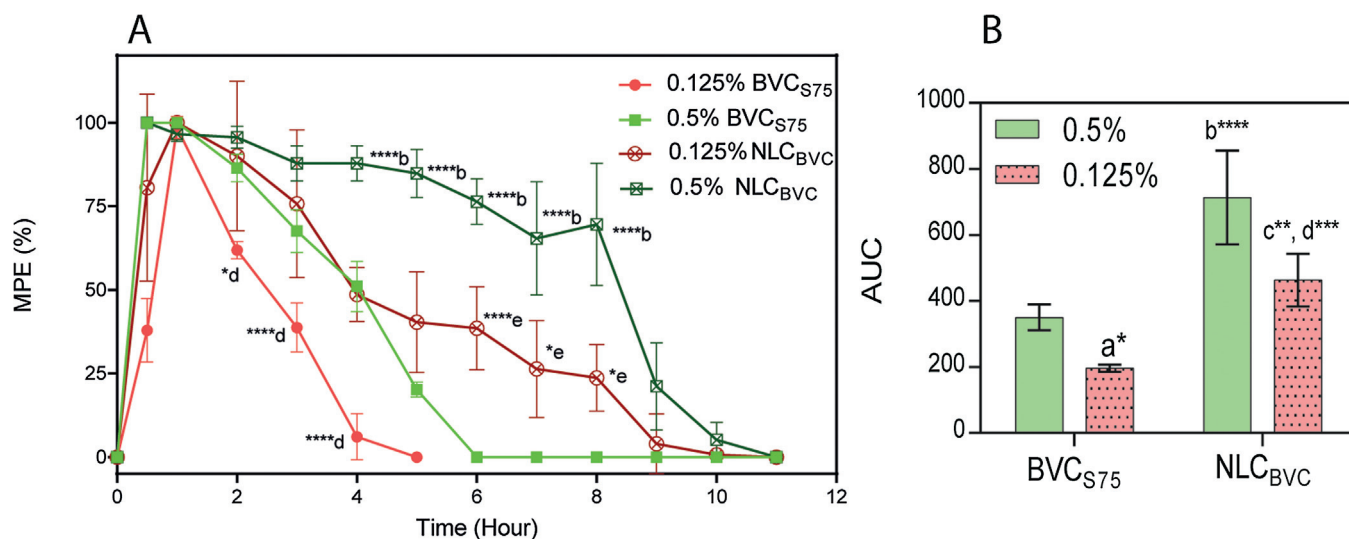
Fig. 8. Anaesthetic (PWPT) test. (A) Maximum possible effect (MPE%) *versus* time for bupivacaine S75:R25 (0.125 and 0.5%) in solution (BVC$_{S75}$) or encapsulated in the optimised nanostructured lipid carriers (NLC$_{BVC}$), n = 5. (B) Area under the curve (effect-time) after injection of bupivacaine S75:R25 in solution (BVC) or encapsulated (NLC$_{BVC}$). Statistical tests One-way ANOVA plus Tukey–Kramer *post hoc*: a, BVC$_{S75}$ 0.125% x BVC$_{S75}$ 0.5%; b, BVC$_{S75}$ 0.5% x NLC$_{BVC}$ 0.5%; c, NLC$_{BVC}$ 0.5% x NLC$_{BVC}$ 0.125%, d, BVC$_{S75}$ 0.125% x NLC$_{BVC}$ 0.125%; e, BVC$_{S75}$ 0.5% x NLC$_{BVC}$ 0.125%. * $p < 0.05$, ***$p < 0.001$, ****$p < 0.0001$.

3.7. 3.7 In vivo *analgesia test by paw pressure tests (PWPT) in rats*

The sciatic nerve block is a test that provides information about the intensity and duration of sensory blockade induced by local anaesthetics in rats (de Araújo et al., 2005; Grillo et al., 2010; Leszczynska and Kau, 1992). The results showing the maximum possible effect induced by BVC$_{S75}$ and NLC$_{BVC}$ sub (0.125%) and normal (0.5%) doses are shown in Fig. 8A. In agreement with the *in vitro* release test, NLC$_{BVC}$ formulations induced longer anaesthesia time in relation to their equivalent (0.125% and 0.5%) solutions of BVC$_{S75}$, confirming the sustained release of bupivacaine. In both NLC formulations (with 0.125% and 0.5% of BVC$_{S75}$), the analgesia time was practically twice as long as that induced by the equivalent anaesthetic solution. Yet at the clinical bupivacaine doses (0.5%) the anaesthetic effect surpassed 8 h when the optimised formulation was administered. In addition, there was no statistically significant difference between 0.5% BVC$_{S75}$ and the NLC$_{BVC}$ formulation at 0.125% bupivacaine, when the area under the curves (AUC) was compared (Fig. 8B). For all tested formulations, there was an initial fast onset of anaesthesia, probably sustained by the non-encapsulated fraction of the drug, which is desirable for a local anaesthetic application (Becker and Reed, 2012). We noticed that, after reaching the maximum possible effect, there was a decrease in the analgesic effect induced by BVC$_{S75}$ in solution, but not by NLC$_{BVC}$, confirming that the anaesthetic remains at the injection site for longer when encapsulated into the nanoparticles.

4. Discussion

Experimental Design indicated the influence of the experimental factors, and their multiple interactions on the properties of the formulation; the optimised parameters were size, polydispersity (PDI) and zeta potential (ZP) (Carbone et al., 2012). For NLC formulations the desired criteria for an optimum formulation included: 1) particles with smaller sizes, which are versatile for parenteral, oral or dermal use (Doktorovová et al., 2016); 2) PDI values ≤ 0.3, and 3) maximised zeta potential values, since, the higher the surface charge (in modulus), the greater the repulsion between the particles, which prevents their aggregation (Chen et al., 2015; Zhang et al., 2009).

The particle size response was directly influenced by the CP concentration, since the viscosity of the lipid phase gets higher at high CP concentrations, making the homogenisation and sonication process less efficient, facilitating the aggregation of the particles and increasing their size (Pradhan et al., 2015). P68 and CAP had the opposite effect, decreasing NLC particles size, being used as surfactant and co-surfactant, respectively. They can both decrease the surface tension between the lipid and the aqueous phase, leading to the formation of smaller sized nanoparticles, and preventing the coalescence of larger droplets (das Neves and Sarmento, 2015). For the same reason, PDI values decreased with the increase of P68 and CAP concentrations. Regarding ZP, the component that negatively influenced this response was P68. P68 is a non-ionic surfactant, that causes depolarisation of the nanoparticles surface, followed by water adsorption, decreasing the zeta potential (Zhao et al., 2014). From the knowledge of how the system behaves in relation to all the experimental variables, it was possible, with the experimental design to select an optimal formulation composed of 9% CP, 4% CAP, 5% P68 and 1% BVC$_{S75}$ (w/ w), also decreasing the overall number of tests.

The optimized formulation presented good encapsulation efficiency (55.5%) for BVC$_{S75}$, and a drug upload of 3.1%. This value is in good agreement with those reported for other local anaesthetic-containing NLC systems: 1.2–2.9% for ropivacaine (Chen et al., 2015) and 1–5% for lidocaine (Nahak et al., 2015). Moreover, the fraction of unbound bupivacaine is expected to contribute in the fast onset of anaesthesia (Becker and Reed, 2012; de Paula et al., 2012).

DSC and XRD analysis showed that the lipid matrix of the nanoparticles was disordered by the addition of CAP and BVC$_{S75}$, as indicated by the decrease in CP fusion enthalpy – from 179.1 J/g in solid lipid nanoparticles to 96.9 J/g NLC$_{FREE}$ and 79.9 J/g for NLC$_{BVC}$ (Fig. 5A), and crystallinity of the solid lipid component (Fig. 5B). This decrease in the lipid organisation is important in the particle architecture, stabilising the NLC and increasing the partition of the anaesthetic, while avoiding its expulsion with time (Puglia et al., 2011), as confirmed by the physicochemical stability results (Fig. 6). Moreover, DSC and XRD results were consistent with the encapsulation of BVC$_{S75}$ (ca. 55%) in the system.

Release kinetic experiments indicated an anomalous non-Fickian transport, as reported by other authors (Nahak et al., 2015;

Neupane et al., 2014; Ribeiro et al., 2016). Thus, in the NLC formulation there is more than one mechanism for BVC_{S75} release, the first caused by the fraction of non-encapsulated drug that has a rapid diffusion, being responsible for the onset of anaesthesia (Becker and Reed, 2012). The second mechanism is that related to the encapsulated drug, responsible for the slow diffusion. After up to 6 h, 70% of the drug was released, representing the fraction of the non-encapsulated drug plus the drug present on the surface of the nanoparticles. After this period, a sustained release rate is kept until the end of the experiment, probably caused by the degradation of the lipid nanoparticles and resulting release of the drug from its matrix (Müller et al., 1996).

The *in vivo* antinociceptive effect (sciatic nerve block) was evaluated through the paw-pressure test, a well-described technique to study the anaesthetic efficiency in rats (Sinnott and Strichartz, 2003). The obtained results (Fig. 8) show that NLC_{BVC} induce longer anaesthesia time than free BVC_{S75}, comprising a prolonged release system, as suggested by the *in vitro* release tests (Fig. 7). In fact improved anaesthesia duration have been observed with other bupivacaine-containing DDS (de Araújo et al., 2005; Shikanov et al., 2007; Grillo et al., 2010; Rogobete et al., 2015). For instance, using the PWPT we have previously shown that the 0.5% BVC_{S75}-HP-beta-cyclodextrin complex increased *ca.* 1.5–1.8 times the anesthesia duration in mice (de Araújo et al., 2005). Also McAlvin and coworkers, using the PWPT to evaluate the sciatic nerve blockade in rats, achieved 4 h anesthesia after injection of a commercial liposome formulation (Exparel™) containing 1.3% bupivacaine (McAlvin et al., 2014).

Here we reached more than 8 h anaesthesia with 0.5% NLC_{BVC} and, in both the concentrations tested (0.125 and 0.5% bupivacaine), the analgesia time with NLC formulations was practically twice that of the anaesthetic in solution (BVC_{S75}). Another important result is that there were no statistically significant differences between the analgesia induced by 0.5% BVC_{S75} and 0.125% NLC_{BVC}. This result is promising and indicates that it is possible to decrease the anaesthetic dose by $1/4$, keeping the same anaesthesia level, so that much less drug could be applied in the clinic, decreasing toxicity.

5. Conclusion

This work describes for the first time, the development of an optimised NLC formulation prepared by experimental design, after the pre-formulation miscibility study carried out by Raman mapping. This last approach opens possibilities for obtaining more information about the NLC components. The optimised formulation showed to be stable for 12 months of storage at room temperature. The analgesic effect of bupivacaine S75:R25 was doubled when it was encapsulated in NLC, reaching the goal of increasing the limited time of action of the local anaesthetic. Moreover, BVC_{S75} doses could be reduced by $1/4$ when encapsulated in NLC, without loss of anaesthesia effect. This formulation is suitable for application by several routes of administration, for different clinical purposes, such as in the prevention of postoperative pain, overcoming the short duration and toxicity associated with bupivacaine use. Thus, its use for topical, parenteral, ocular, intrathecal and intra-articular application can be foreseen.

Declaration of interest

The authors declare they have no conflict of interest.

Acknowledgments

Appendix A. Supplementary data

Supplementary data associated with this article can be found, in the online version, at http://dx.doi.org/10.1016/j.ijpharm.2017.06.066.

References

Abdel-Mottaleb, M.M.A., Neumann, D., Lamprecht, A., 2010. In vitro drug release mechanism from lipid nanocapsules (LNC). Int. J. Pharm. 390, 208–213. doi:http://dx.doi.org/10.1016/j.ijpharm.2010.02.001.

Anantachaisilp, S., Smith, S.M., Treetong, A., Pratontep, S., Puttipipatkhachorn, S., Ruktanonchai, U.R., 2010a. Chemical and structural investigation of lipid nanoparticles: drug-lipid interaction and molecular distribution. Nanotechnology 21, 125102. doi:http://dx.doi.org/10.1088/0957-4484/21/12/125102.

Anantachaisilp, S., Smith, S.M., Treetong, A., Pratontep, S., Puttipipatkhachorn, S., Ruktanonchai, U.R., 2010b. Chemical and structural investigation of lipid nanoparticles: drug-lipid interaction and molecular distribution. Nanotechnology 21, 125102. doi:http://dx.doi.org/10.1088/0957-4484/21/12/125102.

Araújo, J., Gonzalez-Mira, E., Egea, M.A., Garcia, M.L., Souto, E.B., 2010. Optimization and physicochemical characterization of a triamcinolone acetonide-loaded NLC for ocular antiangiogenic applications. Int. J. Pharm. 393, 168–176. doi:http://dx.doi.org/10.1016/j.ijpharm.2010.03.034.

Battaglia, L., Gallarate, M., 2012. Lipid nanoparticles: state of the art, new preparation methods and challenges in drug delivery. Expert Opin. Drug Deliv. 9, 497–508. doi:http://dx.doi.org/10.1517/17425247.2012.673278.

Becker, D.E., Reed, K.L., 2012. Local anesthetics: review of pharmacological considerations. Anesth. Prog. 59, 90–102. doi:http://dx.doi.org/10.2344/0003-3006-59.2.90.

Bergamaschi, F., Balle, V.R., Gomes, M.E.W., Machado, S.B., Mendes, F.F., 2005. Levobupivacaine versus bupivacaine in epidural anesthesia for cesarean section. Comparative study. Rev. Bras. Anestesiol. 55, 606–613. doi:http://dx.doi.org/10.1590/S0034-70942005000600003.

Breitkreitz, M.C., Sabin, G.P., Polla, G., Poppi, R.J., 2013. Characterization of semi-solid self-emulsifying drug delivery systems (SEDDS) of atorvastatin calcium by Raman image spectroscopy and chemometrics. J. Pharm. Biomed. Anal. J. Pharm. Biomed. 73, 3–12. doi:http://dx.doi.org/10.1016/j.jpba.2012.03.054.

Bunjes, H., 2011. Structural properties of solid lipid based colloidal drug delivery systems. Curr. Opin. Colloid Interface Sci. 16, 405–411. doi:http://dx.doi.org/10.1016/j.cocis.2011.06.007.

Carbone, C., Tomasello, B., Ruozi, B., Renis, M., Puglisi, G., 2012. Preparation and optimization of PIT solid lipid nanoparticles via statistical factorial design. Eur. J. Med. Chem. 49, 110–117. doi:http://dx.doi.org/10.1016/j.ejmech.2012.01.001.

Chen, H., Wang, Y., Zhai, Y., Zhai, G., Wang, Z., Liu, J., 2015. Development of a ropivacaine-loaded nanostructured lipid carrier formulation for transdermal delivery. Colloids Surf. A: Physicochem. Eng. Asp. 465, 130–136. doi:http://dx.doi.org/10.1016/j.colsurfa.2014.10.046.

Cheung, E.Y., Harris, K.D.M., Johnston, R.L., Kitchin, S.J., Hadden, K.L., Zakrzewski, M., 2004. Rationalizing the structural properties of bupivacaine base—a local anesthetic—directly from powder X-ray diffraction data. J. Pharm. Sci. 93, 667–674. doi:http://dx.doi.org/10.1002/jps.10551.

Covino, B.G., 1986. Pharmacology of local anaesthetic agents. Br. J. Anaesth. 58, 701–716.

das Neves, J., Sarmento, B., 2015. Precise engineering of dapivirine-loaded nanoparticles for the development of anti-HIV vaginal microbicides. Acta Biomater. 18, 77–87. doi:http://dx.doi.org/10.1016/j.actbio.2015.02.007.

de Araújo, D.R., Fraceto, L.F., Braga, A.F., de Paula, E., 2005. Drug-delivery systems for racemic bupivacaine (S50-R50) and bupivacaine enantiomeric mixture (S75-R25): cyclodextrins complexation effects on sciatic nerve blockade in mice. Rev. Bras. Anestesiol. 55, 316–328. doi:http://dx.doi.org/10.1590/S0034-70942005000300008.

de Melo, N.F.S., Grillo, R., Guilherme, V.A., de Araujo, D.R., de Paula, E., Rosa, A.H., Fraceto, L.F., 2011. Poly(lactide-co-glycolide) nanocapsules containing benzocaine: influence of the composition of the oily nucleus on physico-chemical properties and anesthetic activity. Pharm. Res. 28, 1984–1994. doi:http://dx.doi.org/10.1007/s11095-011-0425-6.

de Paula, E., Cereda, C.M.S., Fraceto, L.F., de Araújo, D.R., Franz-Montan, M., Tofoli, G.R., Ranali, J., Volpato, M.C., Groppo, F.C., 2012. Micro and nanosystems for delivering local anesthetics. Expert Opin. Drug Deliv. 9, 1505–1524. doi:http://dx.doi.org/10.1517/17425247.2012.738664.

Doktorovová, S., Kovačević, A.B., Garcia, M.L., Souto, E.B., 2016. Preclinical safety of solid lipid nanoparticles and nanostructured lipid carriers: current evidence from in vitro and in vivo evaluation. Eur. J. Pharm. Biopharm. 108, 235–252. doi:http://dx.doi.org/10.1016/j.ejpb.2016.08.001.

Garg, A., Bhalala, K., Tomar, D.S., Wahajuddin, 2017. In-situ single pass intestinal permeability and pharmacokinetic study of developed lumefantrine loaded solid lipid nanoparticles. Int. J. Pharm. 516, 120–130. doi:http://dx.doi.org/10.1016/j.ijpharm.2016.10.064.

Gonzalez-Mira, E., Egea, M.A., Souto, E.B., Calpena, A.C., García, M.L., 2011. Optimizing flurbiprofen-loaded NLC by central composite factorial design for ocular delivery. Nanotechnology 22, 45101. doi:http://dx.doi.org/10.1088/0957-4484/22/4/045101.

Grillo, R., de Melo, N.F.S., de Araújo, D.R., de Paula, E., Rosa, A.H., Fraceto, L.F., 2010. Polymeric alginate nanoparticles containing the local anesthetic bupivacaine. J. Drug Target. 18, 688–699. doi:http://dx.doi.org/10.3109/1061186100364738.

Harmatz, A., 2009. Local anesthetics: uses and toxicities. Surg. Clin. N. Am. 89, 587–598. doi:http://dx.doi.org/10.1016/j.suc.2009.03.008.

Hu, F.-Q., Jiang, S.-P., Du, Y.-Z., Yuan, H., Ye, Y.-Q., Zeng, S., 2005. Preparation and characterization of stearic acid nanostructured lipid carriers by solvent diffusion method in an aqueous system. Colloids Surf. B: Biointerfaces 45, 167–173. doi:http://dx.doi.org/10.1016/j.colsurfb.2005.08.005.

ICH, 2009. The International Conference on Harmonization of Technical Requirements for Registration of Pharmaceuticals for Human Use, Quality Guideline Q8(R2) Pharmaceutical Development. .

Joshi, M.D., Müller, R.H., 2009. Lipid nanoparticles for parenteral delivery of actives. Eur. J. Pharm. Biopharm. 71, 161–172. doi:http://dx.doi.org/10.1016/j.ejpb.2008.09.003.

Kasongo, W.A., Pardeike, J., Müller, R.H., Walker, R.B., 2011. Selection and characterization of suitable lipid excipients for use in the manufacture of didanosine-loaded solid lipid nanoparticles and nanostructured lipid carriers. J. Pharm. Sci. 100, 5185–5196. doi:http://dx.doi.org/10.1002/jps.22711.

Korsmeyer, R.W., Gurny, R., Doelker, E., Buri, P., Peppas, N.A., 1983. Mechanisms of solute release from porous hydrophilic polymers. Int. J. Pharm. 15, 25–35. doi:http://dx.doi.org/10.1016/0378-5173(83)90064-9.

Lagan, G., McLure, H.A., 2004. Review of local anaesthetic agents. Curr. Anaesth. Crit. Care 15, 247–254. doi:http://dx.doi.org/10.1016/j.cacc.2004.08.007.

Leszczynska, K., Kau, S.T., 1992. A sciatic nerve blockade method to differentiate drug-induced local anesthesia from neuromuscular blockade in mice. J. Pharmacol. Toxicol. Methods 27, 85–93. doi:http://dx.doi.org/10.1016/1056-8719(92)90026-W.

Müller, R.H., Rühl, D., Runge, S.A., 1996. Biodegradation of solid lipid nanoparticles as a function of lipase incubation time. Int. J. Pharm. 144, 115–121. doi:http://dx.doi.org/10.1016/S0378-5173(96)04731-X.

Müller, R.H., Mäder, K., Gohla, S., 2000. Solid lipid nanoparticles (SLN) for controlled drug delivery—a review of the state of the art. Eur. J. Pharm. Biopharm. 50, 161–177. doi:http://dx.doi.org/10.1016/S0939-6411(00)00087-4.

Müller, R.H., Petersen, R.D., Hommoss, A., Pardeike, J., 2007. Nanostructured lipid carriers (NLC) in cosmetic dermal products. Adv. Drug Deliv. Rev. 59, 522–530. doi:http://dx.doi.org/10.1016/j.addr.2007.04.012.

Müller, R.H., Shegokar, R.M., Keck, C., 2011. 20 years of lipid nanoparticles (SLN & NLC): present state of development & industrial applications. Curr. Drug Discov. Technol. 8, 207–227. doi:http://dx.doi.org/10.2174/157016311796799062.

Martins, S., Tho, I., Reimold, I., Fricker, G., Souto, E., Ferreira, D., Brandl, M., 2012. Brain delivery of camptothecin by means of solid lipid nanoparticles: formulation design, in vitro and in vivo studies. Int. J. Pharm. 439, 49–62. doi:http://dx.doi.org/10.1016/j.ijpharm.2012.09.054.

Mather, L.E., Chang, D.H., 2001. Cardiotoxicity with modern local anaesthetics: is there a safer choice? Drugs 61, 333–342.

McAlvin, J.B., Padera, R.F., Shankarappa, S.A., Reznor, G., Kwon, A.H., Chiang, H.H., Yang, J., Kohane, D.S., 2014. Multivesicular liposomal bupivacaine at the sciatic nerve. Biomaterials 35, 4557–4564. doi:http://dx.doi.org/10.1016/j.biomaterials.2014.02.015.

Mendyk, A., Jachowicz, R., Fijorek, K., Doro, P., Kulinowski, P., Polak, S., Dorożyński, P., Kulinowski, P., Polak, S., 2012. KinetDS: an open source software for dissolution test data analysis. Dissolution Technol. 6–11. doi:http://dx.doi.org/10.14227/DT190112P6.

Mohanty, B., Majumdar, D.K., Mishra, S.K., Panda, A.K., Patnaik, S., 2015. Development and characterization of itraconazole-loaded solid lipid nanoparticles for ocular delivery. Pharm. Dev. Technol. 20, 458–464. doi:http://dx.doi.org/10.3109/10837450.2014.882935.

Moraes, C.M., de Paula, E., Rosa, A.H., Fraceto, L.F., 2008. Validation of analytical methodology by hplc for quantification of bupivacaine (s75-r25) in poli-lactide-co-glicolide nanospheres. Quim. Nova 31, 2152–2155. doi:http://dx.doi.org/10.1590/S0100-40422008000800040.

Nahak, P., Karmakar, G., Roy, B., Guha, P., Sapkota, M., Koirala, S., Chang, C.-H., Panda, A.K., 2015. Physicochemical studies on local anaesthetic loaded second generation nanolipid carriers. RSC Adv. 5, 26061–26070. doi:http://dx.doi.org/10.1039/C4RA16434B.

Neupane, Y.R., Srivastava, M., Ahmad, N., Kumar, N., Bhatnagar, A., Kohli, K., 2014. Lipid based nanocarrier system for the potential oral delivery of decitabine: formulation design, characterization, ex vivo, and in vivo assessment. Int. J. Pharm. 477, 601–612. doi:http://dx.doi.org/10.1016/j.ijpharm.2014.11.001.

Patil, A.S., Pethe, A.M., 2013. Quality by design (QbD): a new concept for development of quality pharmaceuticals. Int. J. Pharm. Qual. Assur. 4, 13–19. doi:http://dx.doi.org/10.1007/s11095-007-9511-1.

Patil-Gadhe, A., Pokharkar, V., 2014. Montelukast-loaded nanostructured lipid carriers: part I oral bioavailability improvement. Eur. J. Pharm. Biopharm. 88, 160–168. doi:http://dx.doi.org/10.1016/j.ejpb.2014.05.019.

Patnaik, P., 2004. Infrared and Raman Spectroscopy. Dean's Anal. Chem. Handbook, second ed. .

Penning, J.P., Yaksh, T.L., 1992. Interaction of intrathecal morphine with bupivacaine and lidocaine in the rat. Anesthesiology 77, 1186–2000.

Pradhan, M., Singh, D., Murthy, S.N., Singh, M.R., 2015. Design, characterization and skin permeating potential of fluocinolone acetonide loaded nanostructured lipid carriers for topical treatment of psoriasis. Steroids 101, 56–63. doi:http://dx.doi.org/10.1016/j.steroids.2015.05.012.

Puglia, C., Sarpietro, M.G., Bonina, F., Castelli, F., Zammataro, M., Chiechio, S., 2011. Development, characterization, and in vitro and in vivo evaluation of benzocaine- and lidocaine-loaded nanostructrured lipid carriers. J. Pharm. Sci. 100, 1892–1899. doi:http://dx.doi.org/10.1002/jps.22416.

Randall, L.O., Selitto, J.J., 1957. A method for measurement of analgesic activity on inflamed tissue. Arch. Int. Pharmacodyn. Thér. CXI 409–419.

Ribeiro, L.N.M., Franz-Montan, M., Breitkreitz, M.C., Alcântara, A.C.S., Castro, S.R., Guilherme, V.A., Barbosa, R.M., de Paula, E., 2016. Nanostructured lipid carriers as robust systems for topical lidocaine-prilocaine release in dentistry. Eur. J. Pharm. Sci. 93, 192–202. doi:http://dx.doi.org/10.1016/j.ejps.2016.08.030.

Ribeiro, L.N.M., Breitkreitzb, M.C., Guilherme, V.A., Rodrigues da Silva, G.H., Verônica, M., Coutoa, S.R.C., Paula, B.O., De Machado, D., de Paula, E., 2017. Natural lipids-based NLC containing lidocaine: from pre-formulation to in vivo studies. Eur. J. Pharm. Sci. 106, 102–112. doi:http://dx.doi.org/10.1016/j.ejps.2017.05.060.

Rogobete, A.F., Bedreag, O.H., Sărăndan, M., Păpurică, M., Preda, G., Dumbuleu, M.C., Vernic, C., Stoicescu, E.R., Săndesc, D., 2015. Liposomal bupivacaine—new trends in anesthesia and intensive care units. Egypt. J. Anaesth. 31, 89–95. doi:http://dx.doi.org/10.1016/j.egja.2014.12.004.

Ruktanonchai, U., Limpakdee, S., Meejoo, S., Sakulkhu, U., Bunyapraphatsara, N., Junyaprasert, V., Puttipipatkhachorn, S., 2008. The effect of cetyl palmitate crystallinity on physical properties of gamma-oryzanol encapsulated in solid lipid nanoparticles. Nanotechnology 19, 95701. doi:http://dx.doi.org/10.1088/0957-4484/19/9/095701.

Rute Neves, A., Lúcio, M., Martins, S., Luís Costa Lima, J., Reis, S., Reis REQUIMTE, S., 2013. Novel resveratrol nanodelivery systems based on lipid nanoparticles to enhance its oral bioavailability. Int. J. Nanomed. 8, 177–187. doi:http://dx.doi.org/10.2147/IJN.S37840.

Sütő, B., Berkó, S., Kozma, G., Kukovecz, Á., Budai-Szucs, M., Erös, G., Kemény, L., Sztojkov-Ivanov, A., Gáspár, R., Csányi, E., 2016. Development of ibuprofen-loaded nanostructured lipid carrier-based gels: characterization and investigation of in vitro and in vivo penetration through the skin. Int. J. Nanomed. 11, 1201–1212. doi:http://dx.doi.org/10.2147/IJN.S99198.

Sabin, G.P., de Souza, A.M., Breitkreitz, M.C., Poppi, R.J., 2012. Development of an algorithm for identification and correction of spikes in raman imaging spectroscopy. Quim. Nova 35, 612–615. doi:http://dx.doi.org/10.1590/S0100-40422012000300030.

Sangshetti, J.N., Deshpande, M., Zaheer, Z., Shinde, D.B., Arote, R., 2017. Quality by design approach: regulatory need. Arab. J. Chem. 10, S3412–S3425. doi:http://dx.doi.org/10.1016/j.arabjc.2014.01.025.

Saupe, A., Gordon, K.C., Rades, T., 2006. Structural investigations on nanoemulsions, solid lipid nanoparticles and nanostructured lipid carriers by cryo-field emission scanning electron microscopy and Raman spectroscopy. Int. J. Pharm. 314, 56–62. doi:http://dx.doi.org/10.1016/j.ijpharm.2006.01.022.

Schwarz, C., Mehnert, W., Lucks, J.S., Müller, R.H., 1994. Solid lipid nanoparticles (SLN) for controlled drug delivery. I. Production, characterization and sterilization. J. Control. Release 30, 83–96. doi:http://dx.doi.org/10.1016/0168-3659(94)90047-7.

Shah, R., Eldridge, D., Palombo, E., Harding, I., 2014. Optimisation and stability assessment of solid lipid nanoparticles using particle size and zeta potential. J. Phys. Sci. 25, 59–75.

Shikanov, A., Domb, A.J., Weiniger, C.F., 2007. Long acting local anesthetic-polymer formulation to prolong the effect of analgesia. J. Control. Release 117, 97–103. doi:http://dx.doi.org/10.1016/j.jconrel.2006.10.014.

Sinnott, C.J., Strichartz, G.R., 2003. Levobupivacaine versus ropivacaine for sciatic nerve block in the rat. Reg. Anesth. Pain Med. 28, 294–303. doi:http://dx.doi.org/10.1016/S1098-7339(03)00188-3.

Souto, E., Wissing, S., Barbosa, C., Müller, R., 2004. Development of a controlled release formulation based on SLN and NLC for topical clotrimazole delivery. Int. J. Pharm. 278, 71–77. doi:http://dx.doi.org/10.1016/j.ijpharm.2004.02.032.

Tauler, R., Smilde, A., Kowalski, B., 1995. Selectivity, local rank, three way data analysis and ambiguity in multivariate curve resolution. J. Chemom. 9, 31–58.

Teeranachaideekul, V., Souto, E.B., Junyaprasert, V.B., Müller, R.H., 2007. Cetyl palmitate-based NLC for topical delivery of coenzyme Q10-development, physicochemical characterization and in vitro release studies. Eur. J. Pharm. Biopharm. 67, 141–148. doi:http://dx.doi.org/10.1016/j.ejpb.2007.01.015.

Tiyaboonchai, W., Tungpradit, W., Plianbangchang, P., 2007. Formulation and characterization of curcuminoids loaded solid lipid nanoparticles. Int. J. Pharm. 337, 299–306. doi:http://dx.doi.org/10.1016/j.ijpharm.2006.12.043.

Vivek, K., Reddy, H., Murthy, R.S.R., 2007. Investigations of the effect of the lipid matrix on drug entrapment, in vitro release, and physical stability of olanzapine-loaded solid lipid nanoparticles. AAPS PharmSciTech 8, 16–24. doi:http://dx.doi.org/10.1208/pt0804083.

Zhang, X., Liu, J., Qiao, H., Liu, H., Ni, J., Zhang, W., Shi, Y., 2009. Formulation optimization of dihydroartemisinin nanostructured lipid carrier using response surface methodology. Powder Technol. 197, 120–128. doi:http://dx.doi.org/10.1016/j.powtec.2009.09.004.

Zhao, S., Yang, X., Garamus, V.M., Handge, U.A., Bérengère, L., Zhao, L., Salamon, G., Willumeit, R., Zou, A., Fan, S., 2014. Mixture of nonionic/ionic surfactants for the formulation of nanostructured lipid carriers: effects on physical properties. Langmuir 30, 6920–6928. doi:http://dx.doi.org/10.1021/la501141m.